

# Positive Stochastic Collocation for the Collocated Local Volatility Model

Fabien Le Floch · Cornelis W. Oosterlee

Received: date / Accepted: date

**Abstract** This paper presents how to apply the stochastic collocation technique to assets that can not move below a boundary. It shows that the polynomial collocation towards a lognormal distribution does not work well. Then, the potentials issues of the related collocated local volatility model (CLV) are explored. Finally, a simple analytical expression for the Dupire local volatility derived from the option prices modelled by stochastic collocation is given.

**Keywords** stochastic collocation · implied volatility · quantitative finance · arbitrage-free · risk neutral density

## 1 Introduction

In the standard Black-Scholes model, the underlying asset follows a geometrical Brownian motion (Black and Scholes 1973). The model is typically applied to obtain the prices and hedges of financial derivative contracts, such as options on a foreign exchange rate, a stock price or a swap rate. For a given maturity date, the market price of a vanilla option for each quoted strike does not match the assumption of a constant Black-Scholes volatility. The volatilities implied by the market exhibit a smile. This is also true in the maturity dimension, where the market implies a particular term-structure of volatilities. Furthermore, the implied volatilities vary in time.

In order to solve this discrepancy, Dupire (1994) proposed a model where the volatility is made local: it is a function of the asset price and a particular time. This model however requires a smooth and continuous arbitrage-free Black-Scholes implied volatility representation across the time and asset price dimensions. Finding a good representation is the principal challenge of this model. The local volatility

---

Fabien Le Floch  
Delft Institute of Applied Mathematics, TU Delft, Delft, The Netherlands  
E-mail: f.l.y.lefloch@tudelft.nl

Cornelis W. Oosterlee, CWI-Centrum Wiskunde & Informatica, Amsterdam, The Netherlands

model also suffers from an unrealistic dynamic of the smile in time (Hagan et al. 2002). In practice this means that forward starting options are mispriced under the local volatility model.

A different approach is to assume that the volatility is stochastic. Several stochastic volatility models that retain some analytical and numerical tractability have been explored over the years, the most popular being the model from Heston (1993). They all suffer from similar issues: they don't allow to match the implied volatility smile for short maturities very well and they can be challenging to calibrate properly. A fix for the former issue is to mix stochastic and local volatilities together (Alexander and Nogueira 2004) at the cost of increasing the computational complexity, which involves either an iterative partial differential equation technique as in (Ren et al. 2007) or the particle method for Monte-Carlo (Guyon and Henry-Labordere 2011; Van der Stoep et al. 2014). A good local volatility representation is a prerequisite for the stochastic local volatility model.

Grzelak (2018) proposes another alternative with the collocated volatility model (CLV), where the model prices are calibrated to the market options with the stochastic collocation technique, used as a convenient representation of the terminal distribution. A specific dynamic is added in the form of a stochastic driver process, which allows more control over the prices of forward starting options. This is reminiscent of the Markov functional model of Hunt and Kennedy (2004), initially derived for interest rate models and extended to equity models in (Fries 2006). How to implement this model for equity derivatives in practice? What are its limitations? Those are a few key questions that we attempt to answer in this paper.

The outline of the paper is as follows. Section 2 introduces the stochastic collocation technique and the CLV model with a Gaussian driver process with time-dependent volatility. We pay attention to explain its relationship with the Markov functional model. Section 3 extends the collocation technique described in (Le Floc'h and Oosterlee 2019) to assets that can not move below a boundary. For example, a stock price must stay positive. This is particularly important as many equity derivative contracts are written on a future performance, and we show that the price of such contracts can not be estimated by a model that allows negative asset prices. Furthermore, we find that the polynomial collocation towards a lognormal distribution does not work well in practice. Section 4 presents how to calibrate the autocorrelation such that the CLV model stays compatible with the assumption of deterministic interest rates, in a similar fashion as Jäckel (2005); Brockhaus (2006) do with the Markov functional model. Finally, in section 5, we show that, with a specific choice of interpolation in time, the stochastic collocation leads to a simple analytical expression for the Dupire local volatility.

## 2 Stochastic collocation and the collocated volatility model

### 2.1 Overview of the stochastic collocation method

The stochastic collocation method (Mathelin and Hussaini 2003) consists in mapping a physical random variable  $Y$  to a point  $X$  of an artificial stochastic space. Collocation

points  $x_i$  are used to approximate the function mapping  $X$  to  $Y$ ,  $F_X^{-1} \circ F_Y$ , typically by a polynomial, where  $F_X, F_Y$  are respectively the cumulative distribution functions (CDF) of  $X$  and  $Y$ . Thus only a small number of inversions of  $Y$  (and evaluations of  $F_Y$ ) are used. This allows the problem to be solved in the "cheaper" artificial space.

In the context of option price interpolation, the stochastic collocation will allow us to interpolate the market CDF in a better set of coordinates. In particular, we will follow [Grzelak and Oosterlee \(2017\)](#) and use a Gaussian distribution for  $X$ .

In ([Grzelak and Oosterlee 2017](#)), the stochastic collocation is applied to the survival distribution function  $G_Y$ , where  $G_Y(y) = 1 - F_Y(y)$  with  $F_Y$  being the cumulative density function of the asset price process. When the survival density function is known for a range of strikes, their method can be summarized by the following steps:

1. Given a set of collocation strikes  $y_i$ ,  $i = 0, \dots, N$ , compute the survival density  $p_i$  at those points:  $p_i = G_Y(y_i)$ .
2. Project on the Gaussian distribution by transforming the  $p_i$  using the inverse cumulative normal distribution  $\Phi^{-1}$  resulting in  $x_i = \Phi^{-1}(1 - p_i)$ .
3. Interpolate  $(x_i, y_i)$  with a Lagrange polynomial  $g_N$ .
4. Price by integrating the density with the integration variable  $x = \Phi^{-1}(1 - G_Y(y))$ , using the Lagrange polynomial for the transform.

Let us now detail the last step. The undiscounted price of an option of strike  $K$  is obtained by integrating over the probability density, with a change of variables,

$$\begin{aligned} C(K) &= \int_0^{+\infty} \max(y - K, 0) f(y) dy & (1) \\ &= \int_{\Phi^{-1}(0)}^{\Phi^{-1}(1)} \max(G_Y^{-1}(1 - \Phi(x)) - K, 0) \phi(x) dx \\ &\approx \int_{-\infty}^{\infty} \max(g_N(x) - K, 0) \phi(x) dx \\ &= \int_{c_K}^{\infty} (g_N(x) - K) \phi(x) dx, & (2) \end{aligned}$$

where  $\phi(x)$  is the Gaussian density function and  $f$  the probability density implied by the options prices and

$$c_K = g_N^{-1}(K). \quad (3)$$

The change of variables is valid when the survival density is continuous and its derivative is integrable. In particular, it is not necessary for the derivative to be continuous.

As shown in ([Hunt and Kennedy 2004](#)), a polynomial multiplied by a Gaussian can be integrated analytically as integration by parts leads to a recurrence relationship on  $m_i(b) = \int_b^{\infty} x^i \phi(x) dx$ . This idea is also the basis of the Sali tree method ([Hu et al. 2006](#)). The recurrence is given by

$$m_{i+2}(b) = (i+1)m_i(b) + b^{i+1}\phi(b), \quad (4)$$

with  $m_0(b) = \Phi(-b)$ ,  $m_1(b) = \phi(b)$ . We have then:

$$C(K) = \sum_{i=0}^N a_i m_i(c_K) - \Phi(-c_K)K, \quad (5)$$

where  $a_i$  are the coefficients of the polynomial in increasing powers.

The terms  $m_i(K)$  involve only  $\phi(c_K)$  and  $\Phi(-c_K)$ . The computational cost for pricing one vanilla option can be approximated by the cost of finding  $c_K$  and the cost of one normal density function evaluation plus one cumulative normal density function evaluation. For cubic polynomials,  $c_K$  can be found analytically through Cardano's formula (Nonweiler 1968) and the cost is similar to the one of the Black-Scholes formula. In the general case of a polynomial  $g_N$  of degree  $N$ , the roots can be computed in  $O(N^3)$  as the eigenvalues of the associated Frobenius companion matrix  $M$  defined by

$$M(g_N) = \begin{pmatrix} 0 & 0 & \dots & 0 & -\frac{a_0}{a_N} \\ 1 & 0 & \dots & 0 & -\frac{a_1}{a_N} \\ 0 & 1 & & 0 & -\frac{a_2}{a_N} \\ \vdots & \vdots & \ddots & \vdots & \vdots \\ 0 & 0 & \dots & 1 & -\frac{a_{N-1}}{a_N} \end{pmatrix}.$$

We have indeed  $\det(\lambda I - M) = g_N(\lambda)$ . This is, for example, how the Octave or Matlab `roots` function works (Moler 1991). Note that for a high degree  $N$ , the system can be very ill-conditioned. A remedy is to use a more robust polynomial basis such as the Chebyshev polynomials and compute the eigenvalues of the colleague matrix (Good 1961; Trefethen 2011). Jenkins and Traub solve directly the problem of finding the roots of a real polynomial in (Jenkins 1975).

A simple alternative, particularly relevant in our case as the polynomial needs to be invertible and thus monotonic, is to use the third-order Halley's method (Gander 1985) with a simple initial guess  $c_K = -1$ , if  $K < F(0, T)$ , or  $c_K = 1$ , if  $K \geq F(0, T)$ , with  $F(0, T)$  the forward price to maturity  $T$ . In practice not more than three iterations are necessary to achieve an accuracy around machine epsilon.

The put option price is calculated through the put-call parity relationship, namely

$$C(K) - P(K) = F(0, T) - K,$$

where  $P(K)$  is the undiscounted price today of a put option of maturity  $T$ , and  $F(0, T)$  is the forward price to maturity.

## 2.2 Collocated Local Volatility with a Gaussian driver process

We consider a dynamic model where

$$X(t) = \sigma_X(t)W(t), \quad (6)$$

$$S(t) = g(t, X(t)), \quad (7)$$

with  $W$  a Brownian motion and  $g$  a collocation function.

Now, from Le Floc'h and Oosterlee (2019), we know how to calibrate the collocation polynomial  $g_N(t_i, z)$  for each maturity independently, on a Gaussian random variable  $Z$  with mean zero and unit standard deviation. The polynomials can be reused in the Monte-Carlo simulation.

Each path followed by the asset  $S$  at times  $(t_i)_{0 < i \leq m}$  in the Monte-Carlo simulation can be computed without any discretization bias, as follows:

- Draw  $m$  independent uniform random numbers  $U_i$ .
- Transform them to Gaussian random numbers  $Z_i = \Phi^{-1}(U_i)$ .
- Compute  $X_i = X_{i-1} + Z_i \sqrt{\int_{t_{i-1}}^{t_i} \sigma_X(v)^2 dv}$ , starting at  $X_0 = 0, t_0 = 0$ .
- Compute  $S(t_i) = g_N(t_i, \frac{X(t_i)}{\sqrt{\int_0^{t_i} \sigma_X(v)^2 dv}})$ .

The underlying idea is not new. It has been proposed by Jäckel (2005) and Brockhaus (2006). Instead of using the collocation on a Gaussian random variable technique, they derive the functional  $g$  from the risk-neutral density, and do not specify a way to imply this risk neutral density. This is often referred to as the Markov functional model, initially derived for interest rate models (Hunt and Kennedy 2004) and extended to equity models in (Fries 2006). Note that the equity Markov functional model uses the equity as the numeraire, so it is not strictly the same. In the CLV model, the functional is directly calibrated to the market.

### 3 Positive collocation

In many applications, the asset can not become negative. But when we apply the stochastic collocation towards a Gaussian variable  $X$ , there is a non-zero probability that the asset  $S$  becomes negative. For example, many exotic equity derivative contracts are written on the future performance  $\frac{S(t_i)}{S(t_j)}$  of the asset. This performance can be computed in a meaningful way only if the asset can not become negative. For example, let us consider the simplest case, a contract paying a future performance  $\frac{S(t_2)}{S(t_1)}$  at  $t_2$ , with  $t_1 < t_2$ . Its value  $V$  at time  $t = 0$  is

$$V(0) = \mathbb{E}_{\mathbb{Q}} \left[ \frac{S(t_2)}{S(t_1)} \right]. \quad (8)$$

Even if the probability that  $S(t_1)$  becomes negative or zero is extremely small, this expectation is not well defined. In practice, when the CLV model with a Gaussian driver of constant volatility is calibrated to three distinct maturities of options on the TSLA stock (table 1), the mean value of a Monte-Carlo simulation of this contract will jump randomly with the number of paths (Figure 1). The standard error never converges to zero.

**Table 1** Coefficients of collocation polynomials calibrated to TSLA options on June 15, 2018.

Expiry	$a_0$	$a_1$	$a_2$	$a_3$	$a_4$	$a_5$
July 20, 2018	356.64	48.632	0.842	-0.565	0.0917	0.412
January 18, 2019	362.86	117.77	-23.49	3.970	5.586	0.729
January 17, 2020	364.01	216.74	-72.76	-29.51	21.83	7.014

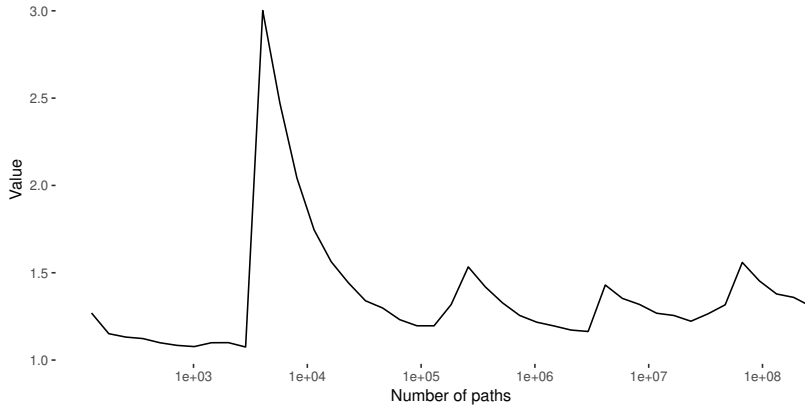


**Fig. 1** Value of a contract on the future performance obtained by Monte-Carlo simulation of a calibrated CLV model, as a function of the number of paths.

### 3.1 Absorption

One remedy is to consider that the density accumulates at  $S = L$  into a discrete probability mass  $p_a$  as in (Grzelak et al. 2018). We obtain  $p_a = \Phi(c_L)$ , with  $c_L = g_N^{-1}(L)$  and the total density over  $[L, +\infty)$  will then still sum to one. The asset will not take any value below  $L$ . In order to ensure strict positivity, we can consider a small but positive  $L$ . It is possible impose the monotonicity of the collocation polynomial and to conserve the first moment in the calibration, while at the same time taking into account this probability mass, by following the technique described in (Le Floc'h and Oosterlee 2019). The first moment is

$$\begin{aligned} F(0, T) &= Lp_a + \int_{c_L}^{\infty} g_N(x)\phi(x)dx \\ &= L\Phi(c_L) + \sum_{i=0}^N a_i m_i(c_L), \end{aligned} \quad (9)$$

with  $m_i$  defined in equation (4). In order to imply  $a_0$  from  $(a_i)_{i \geq 1}$  and  $F(0, T)$ , a one-dimensional non-linear solver is required as  $c_L$  is a function of the coefficient  $a_0$ . The  $a_0$  obtained by integrating from  $-\infty$  to  $\infty$  provides a good initial guess.

In order to price European options, we simply integrate the payoff on  $[L, \infty)$  instead of  $(-\infty, \infty)$ . The call option value is the same as with the standard collocation technique on the polynomial  $g_N$ , for strikes  $K \geq L$ . For  $K < L$ , the undiscounted call option value is the intrinsic value  $F(0, T) - K$ . The resulting fit in terms of implied volatilities is very good, very similar to the standard collocation without absorption. Figure 2 shows the implied volatility when the collocation polynomial is calibrated to TSLA options expiring on January 17, 2020 as of June 15, 2018.

In the collocated local volatility model (CLV) of Grzelak (2018), a dynamic is added to  $X$ , for example  $X$  is a Wiener process and not just a Gaussian random variable. In a Monte-Carlo simulation of the CLV model with absorption, each time-step

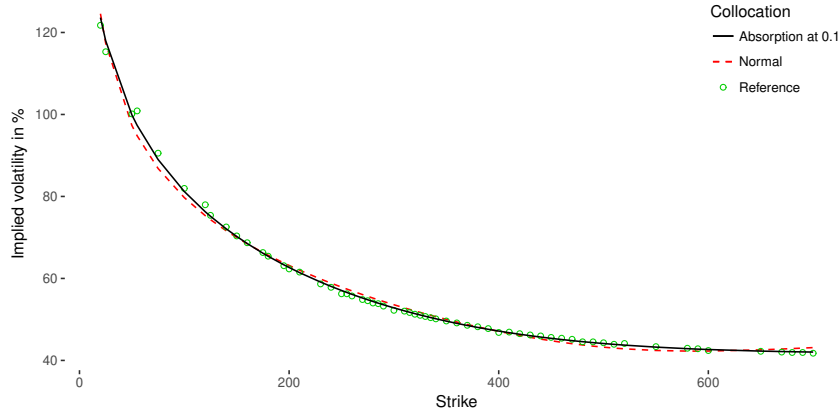


**Fig. 2** Implied volatility obtained from the calibrated quintic collocation polynomial with absorption for TSLA options expiring on January 17, 2020 as of June 15, 2018.

is effectively computed independently of each other and the probability of absorption is already taken into account implicitly in the function  $g_N$ . Unlike a more standard Monte-Carlo simulation of a process with absorption, there is no need to take into account of the eventual absorption at prior times  $t_i < t_j$  for a given observation date  $t_j$ .

Another technique to include absorption is to apply the reflection method (John 1982, p. 220) to the probability density implied by the stochastic polynomial collocation. In this case, the probability of absorption becomes

$$p_a = 2\Phi(c_L) \quad (10)$$

and the first moment is

$$\begin{aligned} F(0, T) &= Lp_a + \int_{c_L}^{\infty} g_N(x)\phi(x)dx - \int_{-\infty}^{c_L} (2L - g_N(x))\phi(x)dx \\ &= \int_{-\infty}^{\infty} g_N(x)dx \\ &= a_0 + \sum_{i=1}^{\frac{N-1}{2}} a_{2i}(2i-1)!!. \end{aligned} \quad (11)$$

In particular, it corresponds to the first moment of the standard polynomial collocation on  $\mathbb{R}$ . Under this absorption model, the undiscounted Call option price is

$$C(K) \approx \int_{c_L}^{\infty} \max(g_N(x) - K, 0)\phi(x)dx - \int_{-\infty}^{c_L} \max(2L - g_N(x) - K, 0)\phi(x)dx. \quad (12)$$

Assuming that  $K > L$ , we have

$$\begin{aligned} C(K) &\approx \int_{c_K}^{\infty} (g_N(x) - K) \phi(x) dx - \int_{-\infty}^{c_{2L-K}} (2L - K - g_N(x)) \phi(x) dx \\ &= \sum_{k=0}^N a_k \left[ m_k(c_K) + (-1)^k m_k(-c_{2L-K}) \right] - \Phi(-c_K)K - (2L - K)\Phi(c_{2L-K}) \end{aligned} \quad (13)$$

with  $c_{2L-K} = g_N^{-1}(2L - K)$ .

With the latter approach, there is no need for a one-dimensional numerical solver in order to include the martingale constraint into the minimization. The Monte-Carlo simulation of the CLV model becomes however slightly more complex, since there is the need to evaluate the payoff on the mirror path as well.

### 3.2 Reflection

Instead of absorption, we can consider that the asset  $S$  reflects at the level  $L$ , and takes the value  $2L - g_N(x)$  for  $x < g_N^{-1}(L)$ . It is still possible to compute the price of a European option analytically. We simply split the integration at  $c_L = g_N^{-1}(L)$ :

$$C(K) \approx \int_{c_L}^{\infty} \max(g_N(x) - K, 0) \phi(x) dx + \int_{-\infty}^{c_L} \max(2L - g_N(x) - K, 0) \phi(x) dx. \quad (14)$$

Assuming that  $K > L$ , we have

$$\begin{aligned} C(K) &\approx \int_{c_K}^{\infty} (g_N(x) - K) \phi(x) dx + \int_{-\infty}^{c_{2L-K}} (2L - K - g_N(x)) \phi(x) dx \\ &= \sum_{k=0}^N a_k \left[ m_k(c_K) - (-1)^k m_k(-c_{2L-K}) \right] - \Phi(-c_K)K + (2L - K)\Phi(c_{2L-K}) \end{aligned} \quad (15)$$

with  $c_{2L-K} = g_N^{-1}(2L - K)$ . We can still calibrate the model while preserving the first moment. With reflection, the first moment is composed of two parts:

$$F(0, T) = \int_{c_L}^{\infty} g_N(x) \phi(x) dx + \int_{-\infty}^{c_L} (2L - g_N(x)) \phi(x) dx, \quad (16)$$

$$= 2L\Phi(c_L) + \sum_{i=0}^N a_i m_i(c_L) - (-1)^i a_i m_i(-c_L). \quad (17)$$

The Monte-Carlo simulation becomes straightforward as there is no dependency on the reflection at previous times. But the model is absolutely not realistic. And in practice, it does not calibrate very well to the market (Figure 3 and Table 2). The preservation of the forward ratio of equation (33) also leads to huge autocorrelation corrections with reflection.



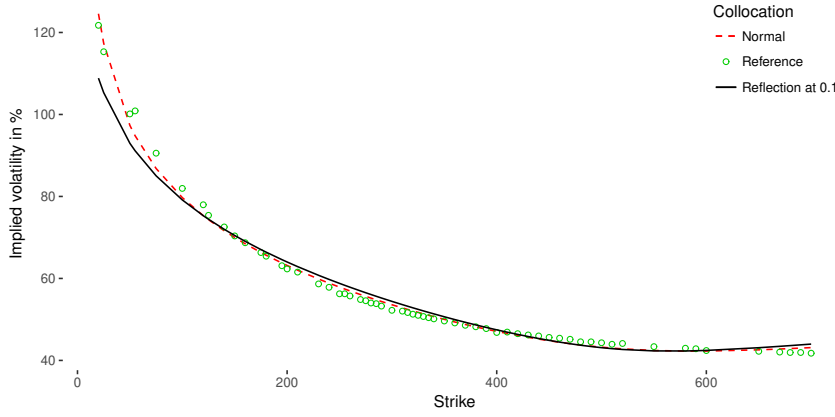


**Fig. 3** Implied volatility obtained from the calibrated quintic collocation polynomial with reflection for TSLA options expiring on January 17, 2020 as of June 15, 2018.

### 3.3 Exponential extrapolation

A simpler alternative is to extrapolate the collocation polynomial with an exponential  $e^{\alpha x + \beta}$  for  $x < x_L$ , where  $x_L$  is chosen so that  $g_N(x_L)$  corresponds to a positive asset price. For example, we can choose the lowest market option strike as extrapolation level. The two parameters  $\alpha$  and  $\beta$  are chosen so that the collocation is of class  $C^1$ :

$$g_N(x_L) = e^{\alpha x_L + \beta}, \quad (18)$$

$$g'_N(x_L) = \alpha e^{\alpha x_L + \beta} = g_N(x_L) \alpha, \quad (19)$$

or equivalently

$$\alpha = \frac{g'_N(x_L)}{g_N(x_L)}, \quad (20)$$

$$\beta = \ln g_N(x_L) - \alpha x_L. \quad (21)$$

As  $g_N$  is strictly increasing and  $g_N(x_L) > 0$  by hypothesis, we have  $\alpha > 0$ . And thus when  $x \rightarrow -\infty$ ,  $e^{\alpha x + \beta} \rightarrow 0$ . The asset can not take a negative value, and all strictly positive values are allowed.

The first moment is now given by

$$\begin{aligned} F(0, T) &= \int_{-\infty}^{x_L} e^{\alpha x + \beta} \phi(x) dx + \int_{x_L}^{\infty} g_N(x) \phi(x) dx \\ &= e^{\beta + \frac{1}{2} \alpha^2} \int_{-\infty}^{x_L} \phi(x - \alpha) dx + \sum_{i=0}^N a_i m_i(x_L) \\ &= e^{\beta + \frac{1}{2} \alpha^2} \Phi(x_L - \alpha) + \sum_{i=0}^N a_i m_i(x_L). \end{aligned} \quad (22)$$

The extrapolation corresponds to a lognormal tail of standard deviation  $\alpha$  as

$$\int_{-\infty}^{x_L} e^{\alpha x + \beta} \phi(x) dx = \int_0^{e^{\alpha x_L + \beta}} z \frac{\phi\left(\frac{\ln z - \beta}{\alpha}\right)}{\alpha z} dz.$$

With the extrapolation, the undiscounted price of a Call option for  $K \geq g_N(x_L)$  is unchanged while the undiscounted price of a Call option for  $K < g_N(x_L)$  reads

$$C(K) = e^{\beta + \frac{1}{2}\alpha^2} (\Phi(x_L - \alpha) - \Phi(c_K - \alpha)) + \sum_{i=0}^N a_i m_i(x_L) - K \Phi(-c_K), \quad (23)$$

where  $c_K = \frac{\ln K - \beta}{\alpha}$ .

The initial guess for the collocation polynomial is the same as without extrapolation. In the non-linear least-squares minimization, the coefficient  $a_0$  is implied from the first moment conservation.

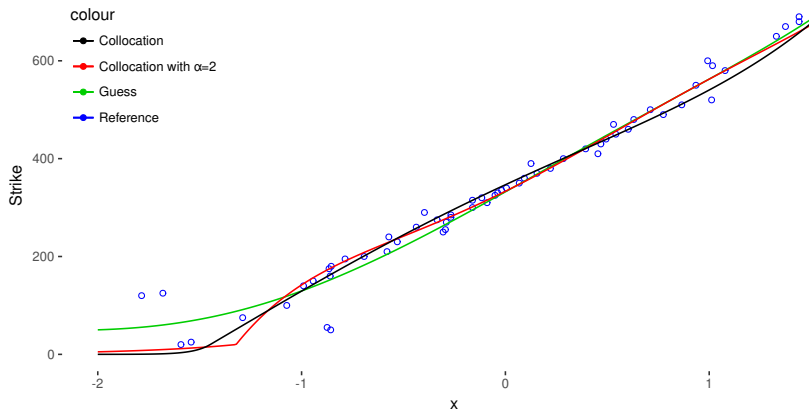


**Fig. 4** Quintic collocation polynomial with exponential extrapolation for TSLA options expiring on January 17, 2020 as of June 15, 2018.

A potential issue is to obtain a too large coefficient  $\alpha$ . In this case, the autocorrelation implied by the Gaussian CLV model will explode. In practice this can happen when the strike cut-off  $g_N(x_L)$  is very low. Two remedies are possible: increase the strike cut-off or cap the coefficient  $\alpha$ , for example to 2.0. In the latter case, we don't impose the continuity of the first derivative of the collocation function anymore and the density will be discontinuous at the cut-off. Figure 4 shows the quintic collocation polynomial with continuous, or capped extrapolation, calibrated to TSLA options expiring on January 17, 2020.

### 3.4 Lognormal collocation

For most financial asset prices, lognormal returns are a typical modelling assumption. It would thus make more sense, a priori, to collocate towards a log-normal random

variable  $X$  with standard deviation  $\sigma_X$ , instead of a normal random variable, using an increasing polynomial map from  $[0, \infty)$  to  $[0, \infty)$ , in a similar fashion as Ware (2019); Boonstra and Oosterlee (2021) do for power prices and the electricity commodity market.

The steps from section 2.1 become:

1. Given a set of collocation strikes  $y_i$ ,  $i = 0, \dots, N$ , compute the survival density  $p_i$  at those points:  $p_i = G_Y(y_i)$ .
2. Project on the log-normal distribution by transforming the  $p_i$  using the inverse cumulative normal distribution  $\Phi^{-1}$  resulting in  $x_i = e^{\sigma_X \Phi^{-1}(1-p_i)}$ .
3. Interpolate  $(x_i, y_i)$  with a monotonically increasing polynomial  $g_N$ .
4. Price by integrating on the density with the integration variable  $x = e^{\sigma_X \Phi^{-1}(1-G_Y(y))}$ , using the Lagrange polynomial for the transform.

Now, the undiscounted price of a vanilla Call option is given by

$$\begin{aligned}
C(K) &= \int_0^\infty \max\left(G_Y^{-1}\left(1 - \Phi\left(\frac{\ln x}{\sigma_X}\right)\right) - K, 0\right) \frac{\phi\left(\frac{\ln x}{\sigma_X}\right)}{\sigma_X x} dx \\
&\approx \int_0^\infty \max(g_N(x) - K, 0) \frac{\phi\left(\frac{\ln x}{\sigma_X}\right)}{\sigma_X x} dx \\
&= \int_{-\infty}^\infty \max(g_N(e^{\sigma_X y}) - K, 0) \phi(y) dy \\
&= \int_{c_K}^\infty (g_N(e^{\sigma_X y}) - K) \phi(y) dy.
\end{aligned} \tag{24}$$

where  $c_K$  is chosen so that  $g_N(e^{\sigma_X c_K}) = K$ . Note that  $c_K$  is not guaranteed to exist anymore as  $\exists K \in \mathbb{R} | g_N^{-1}(K) \leq 0$ . In this case, we take  $c_K$  such that  $g_N(e^{\sigma_X c_K}) = \varepsilon$  with  $\varepsilon$  a small positive real number, typically the machine epsilon.

As in the Gaussian case, the Call price can be computed explicitly:

$$C(K) = \sum_{k=0}^N a_k e^{\frac{1}{2}k^2 \sigma_X^2} \Phi(k\sigma_X - c_K) - K\Phi(-c_K). \tag{25}$$

And the first moment is given by

$$\begin{aligned}
F(0, T) &= \int_{-\infty}^\infty g_N(e^{\sigma_X y}) \phi(y) dy \\
&= \sum_{k=0}^N a_k \int_{-\infty}^\infty e^{k\sigma_X y} \phi(y) dy \\
&= \sum_{k=0}^N a_k e^{\frac{1}{2}k^2 \sigma_X^2}.
\end{aligned} \tag{26}$$

The asset price must stay positive. This implies that  $\forall y \in \mathbb{R}, g_N(e^{\sigma_X y}) > 0$ . By construction, we choose  $g_N$  to be monotonically increasing. And thus we must have  $g_N(0) = a_0 \geq 0$ . In order to allow for all positive asset prices, we must have  $a_0 = 0$ .

From the preservation of the first moment, we imply the first degree monomial coefficient  $a_1$ . The free parameters are then  $a_2, a_3, \dots, a_N$ . Alternatively, we may scale the coefficients  $a_i$  by the ratio of market forward price to theoretical forward price. The isotonic representation of Le Floc'h and Oosterlee (2019) is still applicable, with minor modifications: according to Murray et al. (2016), a polynomial  $p(x)$  of degree  $q$  is non-negative on  $[0, \infty)$  if and only if it can be written as

$$p(x) = p_1(x)^2 + xp_2(x)^2, \quad \forall x \in \mathbb{R},$$

where  $q = 2K$ ,  $p_1(x)$  and  $p_2(x)$  are polynomials whose degrees are at most  $K$  and  $K - 1$  respectively, and, if,  $q = 2K + 1$ , both degrees are at most  $K$ .

In practice however, it turns out not to work very well. A core issue is a lack of invariance in the lognormal collocation.

**Definition 1** A polynomial collocation towards a given distribution  $F_{X, \sigma}$  is invariant with regards to  $\sigma$  if, given a polynomial  $g_1$  and a volatility  $\sigma_1$ , for any  $\sigma_2 > 0$  we can find a collocation polynomial  $g_2$  associated to the volatility  $\sigma_2$  such that  $g_2(x) = g_1(x)$  for all  $x$ .

In the case of the normal distribution,  $g_2$  is simply a scaling factor multiplied by  $g_1$ . In the case of the lognormal distribution, the collocation with  $\sigma_2 \neq \sigma_1$  is fundamentally different, since the polynomial  $g_2$  is applied to  $e^{\sigma_2 x}$  while  $g_1$  is applied to  $e^{\sigma_1 x}$ . We can not reconcile the two unless they are of degree zero. And thus the collocation towards a lognormal variate  $X$  will be very dependent on the choice of the volatility  $\sigma_X$ . In some sense (Equation 24), the basis will effectively be  $(e^{\sigma_X x}, e^{2\sigma_X x}, e^{3\sigma_X x}, \dots)$ , which does not seem particularly appropriate.

If we take  $\sigma_X$  too large, then polynomials will not approximate properly the density: the left tail of  $(x, y)$  behaves like an exponential (Figure 5(a)). If we take  $\sigma_X$  low, the fit is not better: the slope implied by the market data is very large around  $x = 1$ , which would typically make an unconstrained best fit polynomial go through  $(x, 0)$  with  $x$  relatively close to 1, but the condition  $a_0 = 0$  forces the polynomial to pass through the origin, a very different constraint (Figure 5(b)). The polynomial collocation towards a lognormal variable is thus not well suited.

If we relax the positivity constraint and allow  $a_0 \neq 0$ , then the lognormal collocation can fit the market data much better, as long as  $\sigma_X$  is not too large. In figure 6(a) and 6(b), we consider  $\sigma_X = 1$  and  $\sigma_X = \min_{i=0, \dots, m}(\sigma_i \sqrt{T}) \approx 0.547$  where  $\sigma_i$  is the market implied volatility for the option of strike  $K_i$ . When  $\sigma_X$  is too large ( $\sigma_X = 1$  in our example), the unrestricted polynomial still can not fit the market data points. When  $\sigma_X = 0.547$ , a polynomial can fit reasonably well the market data. In terms of implied volatilities, the fit is acceptable (Figure 7).

In order to ensure the positivity of the asset price under collocation, without the constraint  $a_0 = 0$ , we can add an exponential extrapolation, as in the standard normal collocation. The first moment becomes:

$$F(0, T) = e^{\beta + \frac{1}{2}\alpha^2} \Phi(c_L - \alpha) + \sum_{k=0}^N a_k e^{\frac{1}{2}k^2 \sigma_X^2} \Phi(k\sigma_X - c_L), \quad (27)$$

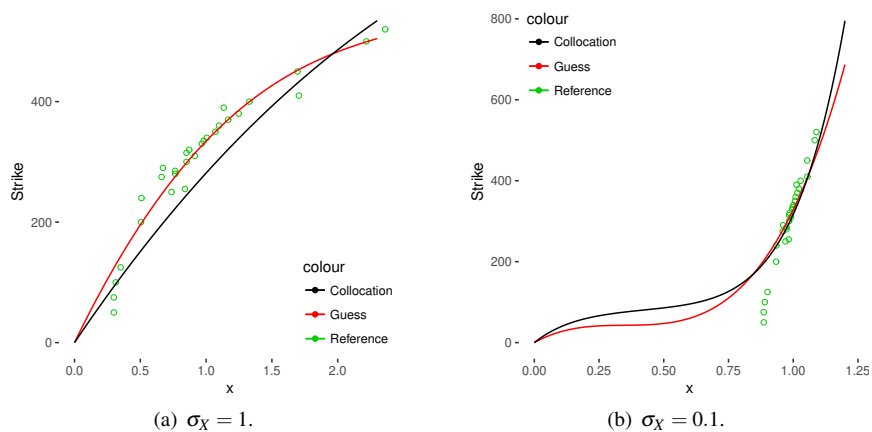


**Fig. 5** Quintic collocation polynomial for a lognormal variable on TSLA options expiring on January 17, 2020 as of June 15, 2018.

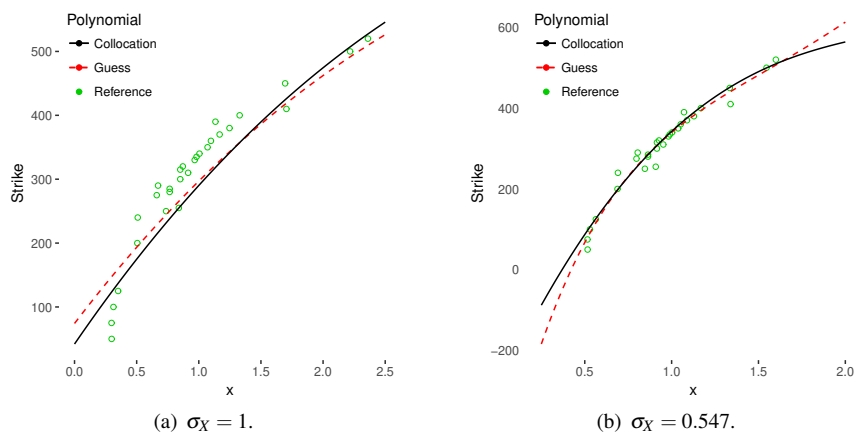


**Fig. 6** Quintic collocation polynomial for a lognormal variable on TSLA options expiring on January 17, 2020 as of June 15, 2018, without the constraint  $a_0 = 0$ .

where  $L$  is a positive cut-off strike and  $c_L = \frac{1}{\sigma_X} \ln g_N^{-1}(L)$ . And when  $K < L$ , the call option price  $C$  becomes

$$C(K) = e^{\beta + \frac{1}{2}\alpha^2} (\Phi(c_L - \alpha) - \Phi(c_K - \alpha)) + \sum_{k=0}^N a_k e^{\frac{1}{2}k^2\sigma_X^2} \Phi(k\sigma_X - c_L) - K\Phi(-c_K), \quad (28)$$

with  $c_K = \frac{\ln(K) - \beta}{\alpha}$ .

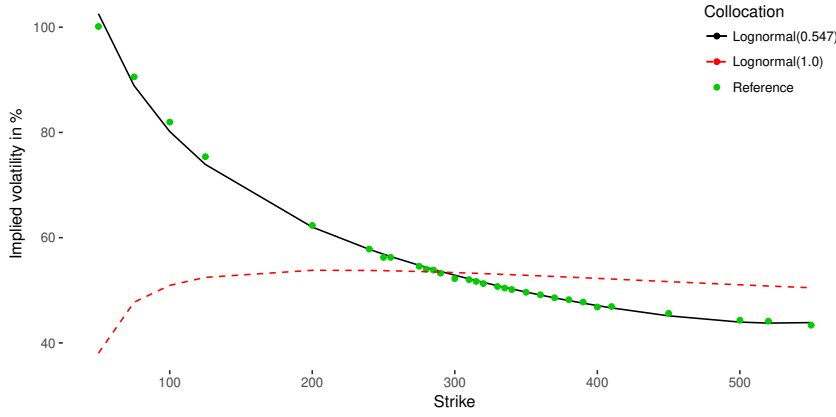


**Fig. 7** Implied volatility obtained from the calibrated unconstrained quintic lognormal collocation polynomial for TSLA options expiring on January 17, 2020 as of June 15, 2018, for two different values of  $\sigma_X$ .

The extrapolation parameters  $\alpha$  and  $\beta$  are determined so that the extrapolation is of class  $C^1$ :

$$g_N(e^{\sigma_X c_L}) = e^{\alpha c_L + \beta}, \quad (29)$$

$$\sigma_X e^{\sigma_X c_L} g'_N(e^{\sigma_X c_L}) = \alpha e^{\alpha c_L + \beta}, \quad (30)$$

or equivalently

$$\alpha = \sigma_X e^{\sigma_X c_L} \frac{g'_N(e^{\sigma_X c_L})}{g_N(e^{\sigma_X c_L})}, \quad (31)$$

$$\beta = \ln g_N(e^{\sigma_X c_L}) - \alpha c_L. \quad (32)$$

As  $g_N$  is strictly monotone and increasing by hypothesis, we have  $g'_N > 0$ . Furthermore, we choose  $c_L$  so that the corresponding strike  $L = g_N(e^{\sigma_X c_L})$  is strictly positive, and the standard deviation  $\sigma_X$  is strictly positive, thus we have  $\alpha > 0$ .

In order to impose the martingality condition, we solve for the coefficient  $a_0$  in equation (27), with a one-dimensional root solver such as Toms348 (Alefeld et al. 1995).

Instead of fixing the standard deviation  $\sigma_X$ , we can use it as an additional calibration parameter in the least squares minimization. This can significantly improve the fit (Figure 8). For the TSLA options expiring on January 17, 2020, the optimal value is  $\sigma_X \approx 0.223$ .

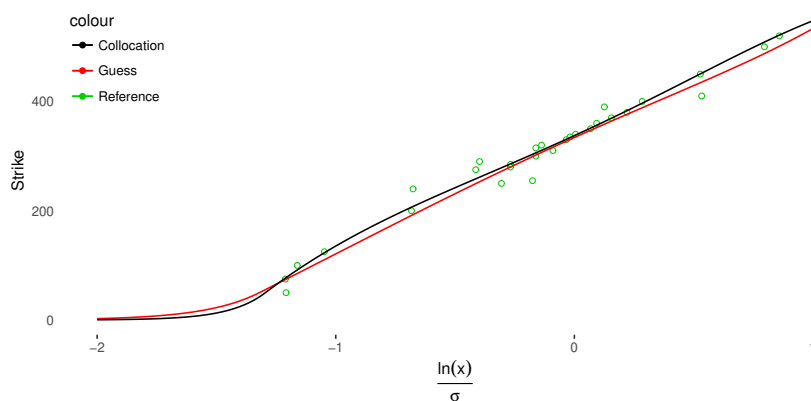


**Fig. 8** Quintic lognormal collocation polynomial with exponential extrapolation for TSLA options expiring on January 17, 2020 as of June 15, 2018. The final lognormal standard deviation is chosen in order to minimize the least-squares error in option prices, with an initial lognormal standard deviation  $\sigma = 0.547$ .

**Table 2** Root mean square error (RMSE) in implied volatilities obtained by various collocation methods on TSLA options of maturity January 17, 2020.

Collocation method	RMSE
Normal	0.0142
Absorption	0.0073
Reflection	0.0302
Exponential extrapolation with optimal $\alpha = 13.4$	0.0064
Exponential extrapolation with capped $\alpha = 2$	0.0077
Lognormal with min. vol $\sigma = 0.527$	0.0227
Lognormal with optimal $\sigma = 0.144$	0.0173
Lognormal with min. vol $\sigma = 0.527$ and optimal $\alpha = 11.3$	0.0067
Lognormal with optimal $\sigma = 0.091$ and optimal $\alpha = 13$	0.0052
Lognormal with optimal $\sigma = 0.0545$ and capped $\alpha = 2$	0.0177

## 4 Calibration of the autocorrelation in the CLV model

### 4.1 The drift in the CLV model

With an arithmetic Brownian driver process<sup>1</sup>, the CLV model from Grzelak (2018) does not respect

$$\mathbb{E}_{\mathbb{Q}} \left[ \frac{S_i}{S_j} \right] = \frac{F_i}{F_j}. \quad (33)$$

It is thus not compatible with an assumption of deterministic interest rates. In fact, when the asset is used as the numeraire, the value  $\mathbb{E}_{\mathbb{Q}} \left[ \frac{S_i}{S_j} \right]$  implies an inherent stochastic interest rate behaviour, for which there is reason to be in line with the market (Fries 2006).

<sup>1</sup> This extends to more sophisticated processes such as the Ornstein-Uhlenbeck process

The presence of a spurious drift can be deduced from the application of the Itô Lemma:

$$dS = \left( \frac{\partial g}{\partial t} + \frac{\sigma_X(t)^2}{2} \frac{\partial^2 g}{\partial x^2} \right) dt + \sigma_X(t) \frac{\partial g}{\partial x} dW(t), \quad (34)$$

the drift is not zero in general. Carr et al. (1999) have shown that imposing  $\frac{\partial g}{\partial t} + \frac{\sigma_X(t)^2}{2} \frac{\partial^2 g}{\partial x^2} = 0, \forall t > 0, \forall x \in \mathbb{R}$ , is a very restrictive condition on  $g$ .

#### 4.2 Calibration of the autocorrelation

Similarly to the Markov functional model, for a given discretization, it is possible to force a specific autocorrelation of the driver process in order to match  $\mathbb{E} \left[ \frac{S_i}{S_j} \right] = \frac{F_i}{F_j}$ , as long as the process  $S$  is guaranteed to stay strictly positive.

With the driver  $X(t) = \sigma_X(t)W(t)$ , for  $t_i < t_j$ , assuming that  $\sigma_X(t) > 0$ , the autocorrelation reads

$$\rho_{i,j} = \frac{\mathbb{E}[X(t_i)X(t_j)]}{\sqrt{\int_0^{t_i} \sigma_X(u)^2 du \int_0^{t_j} \sigma_X(u)^2 du}} = \sqrt{\frac{\int_0^{t_i} \sigma_X(u)^2 du}{\int_0^{t_j} \sigma_X(u)^2 du}}. \quad (35)$$

In particular, for a Brownian motion, when  $\sigma_X$  is constant, we have

$$\rho_{i,j} = \sqrt{\frac{t_i}{t_j}}.$$

Instead of this autocorrelation, as in (Jäckel 2005; Brockhaus 2006), we choose a specific autocorrelation  $\rho_{i,j}$  such that the deterministic forward ratio is preserved:

$$\mathbb{E}_{\mathbb{Q}} \left[ \frac{S_j}{S_i} \right] = \frac{F(0, t_j)}{F(0, t_i)}. \quad (36)$$

The expectation can be computed in closed form. We have

$$\mathbb{E}_{\mathbb{Q}} \left[ \frac{S_j}{S_i} \right] = \int_{-\infty}^{\infty} \int_{-\infty}^{\infty} \frac{g(t_j, \rho_{i,j}u + \sqrt{1 - \rho_{i,j}^2}v)}{g(t_i, v)} \phi(u)\phi(v) dudv. \quad (37)$$

If we integrate first on the variable  $u$ , the inner integral has an explicit formula in terms of the normal cumulative function  $\Phi$  in a similar fashion as for the first moment. For the Gaussian collocation with exponential extrapolation, we obtain:

$$\begin{aligned} \mathbb{E}_{\mathbb{Q}} \left[ \frac{S_j}{S_i} \right] &= \int_{-\infty}^{\infty} \frac{e^{\frac{1}{2}\alpha^2 \bar{\rho}_{i,j}^2 + \alpha \rho v + \beta} \Phi(c(v) - \alpha \bar{\rho}_{i,j})}{g(t_i, v)} \phi(v) dv \\ &+ \int_{-\infty}^{\infty} \frac{\sum_{k=0}^N a_k(t_j) \sum_{l=0}^k \binom{k}{l} \bar{\rho}_{i,j}^l \rho_{i,j}^{k-l} v^{k-l} m_l(c(v))}{g(t_i, v)} \phi(v) dv, \end{aligned} \quad (38)$$



with  $c(v) = \frac{c_L - \rho_{i,j} v}{\bar{\rho}_{i,j}}$ ,  $\bar{\rho}_{i,j} = \sqrt{1 - \rho_{i,j}^2}$ ,  $c_L = g^{-1}(t_j, L)$ ,  $L$  is the extrapolation cut-off strike, and  $a_k(t_j)$  are the coefficient of the  $k$ -th monomial of  $g_N(t_j)$ . The outer integral can be computed with an adaptive Gauss-Lobatto quadrature.

We can thus calibrate the  $\rho_{i,j}$  for  $t_i < t_j$  to deterministic forward ratios. The constant Gaussian driver autocorrelation can be used as initial guess.

Alternatively, from equation (35), we could also calibrate a piecewise constant volatility parameter  $\sigma_X(t)$  approximately to the deterministic forward ratios (in this case there are  $m$  constants to calibrate against  $m \cdot \frac{m-1}{2}$  forward ratios, where  $m$  is the number of time-steps).

The autocorrelations lead to the following correlation matrix  $A$  relating normal variates to the path values on the normalized coordinate  $x$ :

$$A \cdot \begin{pmatrix} z_1 \\ z_2 \\ z_3 \\ \vdots \\ z_m \end{pmatrix} = \begin{pmatrix} x_1 \\ x_2 \\ x_3 \\ \vdots \\ x_m \end{pmatrix}. \quad (39)$$

with

$$AA^T = \begin{pmatrix} 1 & \rho_{1,2} & \rho_{1,3} & \cdots & \rho_{1,m} \\ \rho_{1,2} & 1 & \rho_{2,3} & \cdots & \rho_{2,m} \\ \rho_{1,3} & \rho_{2,3} & 1 & \cdots & \rho_{3,m} \\ \vdots & & & \ddots & \vdots \\ \rho_{1,m} & \rho_{2,m} & \rho_{3,m} & \cdots & 1 \end{pmatrix} \quad (40)$$

The correlation matrix exists only if the covariance matrix is positive definite and can be computed by Cholesky decomposition or by singular value decomposition (SVD). The latter allows to compute an reasonably good approximative correlation matrix even if the original covariance matrix is not positive definite (Jäckel 2004).

In the Monte-Carlo simulation, we then compute each path according to the following steps:

- Draw  $m$  independent uniform random numbers  $U_i$ .
- Transform them to Gaussian random numbers  $Z_i = \Phi^{-1}(U_i)$ .
- Compute  $X_i = \sum_{j=1}^m A_{i,j} Z_j$ .
- Compute  $S(t_i) = g_N(t_i, X_i)$ .

### 4.3 A refined criteria

Brockhaus (2006) proposes a more general identity than the forward ratio in the absence of arbitrage. In order to match the behavior with deterministic interest rates, we must have

$$\mathbb{E}_{\mathbb{Q}} \left[ \frac{S_j}{S_i} 1_{S_i > B} \right] = \frac{F(0, t_j)}{F(0, t_i)} P(S_i > B), \quad (41)$$

where  $B$  is a barrier level, and  $P(S_i > B)$  is the probability that the asset  $S$  is above  $B$  at time  $t_i$ . With the CLV model, this can still be computed in closed form:

$$\mathbb{E}_{\mathbb{Q}} \left[ \frac{S_j}{S_i} 1_{S_i > B} \right] = \int_{c_B}^{\infty} \int_{-\infty}^{\infty} \frac{g(t_j, \rho_{i,j} u + \sqrt{1 - \rho_{i,j}^2} v)}{g(t_i, v)} \phi(u) \phi(v) du dv, \quad (42)$$

where  $c_B = g^{-1}(t_i, B)$ . And, for the standard collocation, we also have

$$P(S_i > B) = \Phi(-c_B), \quad (43)$$

for  $B \geq L$  in the case of an extrapolation cut-off at  $L$ .

#### 4.4 Numerical example on TSLA options

On the 15th of June 2018, we consider options on the TSLA stock at three distinct maturities: July 20, 2018 (1 month), January 18, 2019 (7 months), January 17, 2020 (19 months). We calibrate quintic collocation polynomials with exponential extrapolation to this data. This results in the implied volatility smiles of Figure 9. The fit for each option maturity is excellent.

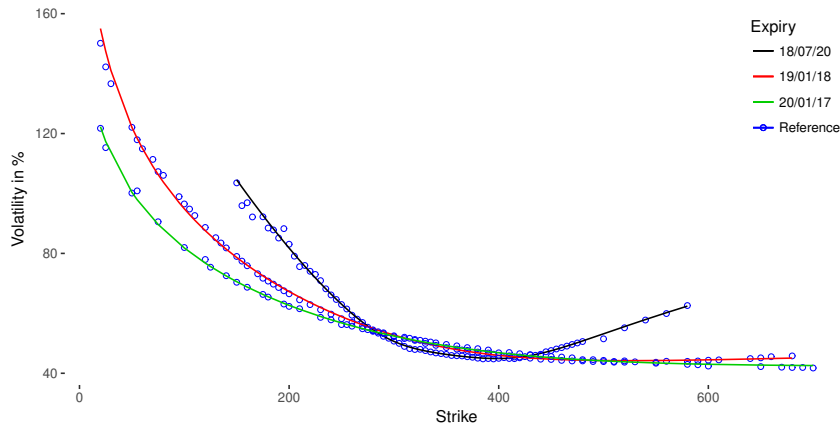


**Fig. 9** Implied volatility smiles obtained by quintic collocation with exponential extrapolation for TSLA options as of June 15, 2018.

In table 3, we then compute the optimal autocorrelations to preserve the deterministic forward ratios between each maturity according to equation (37).

Finally, in table 4, we verify with a Monte-Carlo simulation that the calibrated autocorrelations allow to preserve the forward ratios, and compare with the raw autocorrelations of a Wiener process with constant volatility. In particular, we observe a significant drift of the forward without calibration of the autocorrelations. This is much more pronounced without cap on the  $\alpha$  extrapolation parameter in the collocation polynomial calibration, but is still important with a relatively low cap. The

**Table 3** Autocorrelations between option maturities. The indices 1, 2, 3 denote the first, second and third option maturities.

Autocorrelation method	$\rho_{1,2}$	$\rho_{1,3}$	$\rho_{2,3}$
Wiener	0.4016	0.2454	0.6111
Calibrated	0.4017	0.2531	0.9061
Calibrated with $\alpha$ capped to 2	0.4021	0.2505	0.7743

**Table 4** Monte-Carlo simulation of the contract on the ratio  $\frac{S(t_3)}{S(t_2)}$  with 4 million paths. The deterministic value is 1.0017

Autocorrelation method	Monte-Carlo mean (std. err)	Error	Analytical value
$\alpha$ uncapped			
Wiener	13484.071 ( $\pm$ 4911)	13483.0700	$2.74 \cdot 10^7$
Calibrated	0.966 ( $\pm$ 0.007)	-0.0360	1.0017
$\alpha$ capped to 2			
Wiener	1.1606 ( $\pm$ 0.0013)	0.1589	1.1607
Calibrated	1.0017 ( $\pm$ 0.0005)	0.0000	1.0017

autocorrelations adjustment does not work as well for the uncapped exponential extrapolation, because with a large extrapolation factor  $\alpha$ , the extrapolation is very close to zero for relatively small negative values of  $x$ . This creates an instability in the Monte-Carlo simulation as the asset almost reaches zero too quickly.

The CLV model with adjusted autocorrelation does not lead to an easy PDE representation. It is much simpler to consider a term-structure of volatilities for the driver process instead, which will allow to match approximately the forward ratios between each expiries.

We calibrate a term structure of piecewise constant forward volatilities for the driver process, instead of the direct individual autocorrelation, with only three maturities. Let the forward volatility be  $\sigma_k$  between  $t_k$  and  $t_{k+1}$ , the total variance up to a time  $t_i$  is then

$$\int_0^{t_i} \sigma_X^2(u) du = \sum_{k=1}^i \sigma_{k-1}^2 (t_k - t_{k-1}), \quad (44)$$

with  $t_0 = 0$ . In particular, it is guaranteed to increase, and thus the model is well defined, in contrast to the approach of Brockhaus (2006). The choice of the first volatility parameter  $\sigma_0$  is free, we take simply  $\sigma_0 = 1.0$  and calibrate  $\sigma_1$  and  $\sigma_2$  to the forward ratios  $\mathbb{E}_{\mathbb{Q}} \left[ \frac{S_2}{S_1} \right]$ ,  $\mathbb{E}_{\mathbb{Q}} \left[ \frac{S_3}{S_1} \right]$ ,  $\mathbb{E}_{\mathbb{Q}} \left[ \frac{S_3}{S_2} \right]$ .

With the capped extrapolation, we find a solution that is close to the three forward ratios (Table 5). On our example, there are two forward volatilities to calibrate to

**Table 5** Forward volatilities calibrated to the forward ratios.  $e_{i,j}$  is the error in the forward ratio  $\mathbb{E}_{\mathbb{Q}} \left[ \frac{S_j}{S_i} \right]$ .

$\sigma_1$	$\sigma_2$	$e_{1,2}$	$e_{1,3}$	$e_{2,3}$
1.154	0.714	0.0030	-0.0025	0.0001

three forward ratios. In the more general case, there are  $n - 1$  forward volatilities to calibrate to  $\frac{n(n-1)}{2}$  forward ratios, and thus with more expiries, the error in the forward ratios is likely to be larger.

With the calibrated autocorrelations, we can also evaluate the error of the refined criteria described in section 4.3. On Figure 10, we plot the relative error in the price of the forward performance  $\frac{S_3}{S_2}$  with barrier at  $B$ , varying  $B$ . For relatively low strikes, the

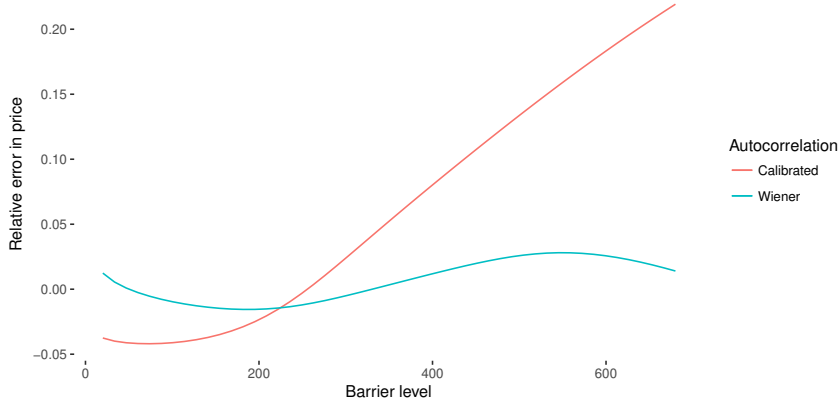


**Fig. 10** Relative error in the forward performance  $\frac{S_3}{S_2}$  with barrier at  $B$ , varying  $B$  for the collocation with capped extrapolation.

error can be of around 5% and for large strikes, it can be even higher. This is in line with Brockhaus (2006) observations, and is the drawback of the CLV or the Markov functional models applied to equities. When the autocorrelation is not calibrated, the relative error in the forward performance with barrier is actually smaller, below 3%. But without barrier, the relative error reaches 16% as shown in Table 4. Regarding the effect of autocorrelation and the calibration to the forward performance, the lognormal collocation behaves the same way as the collocation towards a Gaussian random variable.

In comparison, the local volatility model is fully consistent, but offers no control over forward smile dynamic, which is unrealistic.

## 5 Local volatility for a term-structure of collocated smiles

Gatheral and Jacquier (2014) present the discrete version of the calendar spread no-arbitrage condition:

$$\frac{C(K_2, T_2)}{K_2} \geq \frac{C(K_1, T_1)}{K_1} \quad (45)$$

for  $T_2 \geq T_1$ , where  $C$  is the undiscounted call option price and the strikes  $K_2, K_1$  are chosen so that the forward moneyness is constant:

$$\frac{K_1}{F(0, T_1)} = \frac{K_2}{F(0, T_2)}.$$

This can be derived from Jensen inequality, knowing that the process  $\frac{S(t)}{F(0,t)}$  is a martingale.

This discrete arbitrage-free inequality can be used to define an arbitrage-free interpolation in time assuming that it is verified at two expiries  $t_1$  and  $t_2$ . For example, we can define the prices at time  $t_1 < t < t_2$  by

$$C(K, t) = \frac{t-t_1}{t_2-t_1} \frac{F(0,t)}{F(0,t_2)} C\left(\frac{KF(0,t_2)}{F(0,t)}, t_2\right) + \frac{t_2-t}{t_2-t_1} \frac{F(0,t)}{F(0,t_1)} C\left(\frac{KF(0,t_1)}{F(0,t)}, t_1\right). \quad (46)$$

Dupire (1994) expresses the local volatility  $\sigma_L$  as:

$$\sigma_L^2(K, T) = 2 \frac{\frac{\partial C_0}{\partial T}}{K^2 \frac{\partial^2 C_0}{\partial K^2}}, \quad (47)$$

where  $C_0(K, T)$  is the undiscounted call option price on a fixed forward  $F(0, T)$ . With the collocation method, the Dupire local volatility has a closed form expression with the above interpolation of Call prices in time.

$$\frac{\partial C_0}{\partial T}(K, t) = \frac{K}{t_2-t_1} \left( \frac{C(K_2, t_2)}{K_2} - \frac{C(K_1, t_1)}{K_1} \right) \quad (48)$$

for  $\frac{K}{F(0,t)} = \frac{K_1}{F(0,t_1)} = \frac{K_2}{F(0,t_2)}$ .

$$\frac{\partial^2 C_0}{\partial K^2}(K, t) = \frac{t-t_1}{t_2-t_1} \frac{K_2}{K} \frac{\partial^2 C}{\partial K^2}(K_2, t_2) + \frac{t_2-t}{t_2-t_1} \frac{K_1}{K} \frac{\partial^2 C}{\partial K^2}(K_1, t_1). \quad (49)$$

When the call option prices are determined by the collocation method with a function  $g_N$ , we have

$$\frac{\partial C}{\partial K}(K_i) = -\Phi(-c_{K_i}), \quad \frac{\partial^2 C}{\partial K^2}(K_i) = \frac{\phi(c_{K_i})}{g_{iN}'(c_{K_i})}, \quad (50)$$

with  $c_{K_i} = g_{iN}^{-1}(K_i)$ . For  $t_1 < t < t_2$ , the Dupire equation becomes

$$\sigma_L(K, t) = 2K^2 \frac{\frac{C(K_2, t_2)}{K_2} - \frac{C(K_1, t_1)}{K_1}}{(t-t_1)K_2 \frac{\phi(c_{K_2})}{g_{2N}'(c_{K_2})} + (t_2-t)K_1 \frac{\phi(c_{K_1})}{g_{1N}'(c_{K_1})}}. \quad (51)$$

## 6 Conclusion

Among the various ways to apply the stochastic collocation technique to represent the prices of vanilla options on an asset constrained above boundary, we found that absorption and exponential extrapolation were preferable, for their simplicity and their ability to fit the market, while the polynomial collocation towards a lognormal distribution was much less adequate in practice, partly because of its strong dependency on the choice of lognormal volatility.

We also explained that the CLV model does not respect some key identities linked to the future performance under the assumption of deterministic interest rates, as well as the amplitude of the discrepancies. While this could be considered as a barrier to the use of such a model, it is not necessarily worse than the popular Dupire local volatility model. The Dupire local volatility model is consistent with regards to those identities, but suffers from a bad forward smile dynamic, and will thus give particularly bad prices for contracts written on a future performance. The CLV model allows some flexibility towards the capture of this forward smile dynamic, which could be more in line with the market of forward starting (or barrier) options, but suffers from those other discrepancies.

Finally, we have shown that the stochastic collocation technique can also be interesting to use as a basis to obtain a smooth Dupire local volatility, for example in the context of a stochastic volatility model.

## References

- Alefeld G, Potra FA, Shi Y (1995) Algorithm 748: enclosing zeros of continuous functions. *ACM Transactions on Mathematical Software (TOMS)* 21(3):327–344
- Alexander C, Nogueira L (2004) Hedging with stochastic and local volatility. Tech. rep., Henley Business School, Reading University
- Black F, Scholes M (1973) The pricing of options and corporate liabilities. *Journal of political economy* 81(3):637–654
- Boonstra BC, Oosterlee CW (2021) Valuation of electricity storage contracts using the cos method. *Applied Mathematics and Computation* 410:126416
- Brockhaus O (2006) Implied sampling: Properties and pitfalls. Commerzbank
- Carr P, Tari M, Zariphopoulou T (1999) Closed form option valuation with smiles. Preprint NationsBanc Montgomery Securities
- Dupire B (1994) Pricing with a smile. *Risk* 7(1):18–20
- Fries CP (2006) Markov functional modeling of equity, commodity and other assets
- Gander W (1985) On halley's iteration method. *American Mathematical Monthly* pp 131–134
- Gatheral J, Jacquier A (2014) Arbitrage-free svi volatility surfaces. *Quantitative Finance* 14(1):59–71
- Good I (1961) The colleague matrix, a chebyshev analogue of the companion matrix. *The Quarterly Journal of Mathematics* 12(1):61–68
- Grzelak L, Witteveen J, Suarez-Taboada M, Oosterlee C (2018) The stochastic collocation monte carlo sampler: highly efficient sampling from 'expensive' distributions. *Quantitative Finance* pp 1–18
- Grzelak LA (2018) The collocating local volatility framework – a fresh look at efficient pricing with smile. *International Journal of Computer Mathematics* 0(0):1–20, DOI 10.1080/00207160.2018.1547378, URL <https://doi.org/10.1080/00207160.2018.1547378>
- Grzelak LA, Oosterlee CW (2017) From arbitrage to arbitrage-free implied volatilities. *Journal of Computational Finance* 20(3):31–49
- Guyon J, Henry-Labordere P (2011) The smile calibration problem solved. Available at SSRN 1885032
- Hagan PS, Kumar D, Lesniewski AS, Woodward DE (2002) Managing smile risk. *Wilmott magazine*
- Heston SL (1993) A closed-form solution for options with stochastic volatility with applications to bond and currency options. *Review of financial studies* 6(2):327–343
- Hu Z, Kerkhof J, McCloud P, Wackertapp J (2006) Cutting edges using domain integration. *Risk* 19(11):95
- Hunt P, Kennedy J (2004) *Financial derivatives in theory and practice*. John Wiley & Sons
- Jäckel P (2004) *Monte Carlo methods in finance*, reprint. with corr., september 2004 edn. Wiley finance series, Wiley
- Jäckel P (2005) A practical method for the valuation of a variety of hybrid products. In: ICBI conference slides
- Jenkins MA (1975) Algorithm 493: Zeros of a real polynomial [c2]. *ACM Transactions on Mathematical Software (TOMS)* 1(2):178–189
- John F (1982) *Partial differential equations*, volume 1 of applied mathematical sciences

- Le Floc'h F, Oosterlee CW (2019) Model-free stochastic collocation for an arbitrage-free implied volatility: Part i. *Decisions in Economics and Finance* DOI 10.1007/s10203-019-00238-x, URL <https://doi.org/10.1007/s10203-019-00238-x>
- Mathelin L, Hussaini MY (2003) A stochastic collocation algorithm for uncertainty analysis. NASA CR-2003-212153
- Moler C (1991) Cleve's corner: Roots-of polynomials, that is. *The MathWorks Newsletter* 5(1):8–9
- Murray K, Müller S, Turlach B (2016) Fast and flexible methods for monotone polynomial fitting. *Journal of Statistical Computation and Simulation* 86(15):2946–2966
- Nonweiler TR (1968) Algorithms: Algorithm 326: Roots of low-order polynomial equations. *Communications of the ACM* 11(4):269–270
- Ren Y, Madan D, Qian MQ (2007) Calibrating and pricing with embedded local volatility models. *RISK-LONDON-RISK MAGAZINE LIMITED*- 20(9):138
- Van der Stoep AW, Grzelak LA, Oosterlee CW (2014) The heston stochastic-local volatility model: efficient monte carlo simulation. *International Journal of Theoretical and Applied Finance* 17(07):1450045
- Trefethen LN (2011) Six myths of polynomial interpolation and quadrature. Tech. rep., *Mathematics Today*
- Ware T (2019) Polynomial processes for power prices. *Applied Mathematical Finance* 26(5):453–474